Nuclear magnetic resonance

First sight of a single cell

from John Mallard

A PAPER on page 190 of this issue[1] describes the first nuclear magnetic resonance (NMR) images of a single cell. This offers the exciting possibility of fine-resolution NMR imaging of cells and collections of cells. The magnetic-field strengths which are used in clinical imaging range from 0.02 to 1 tesla, with about 0.1–0.5 tesla being the norm, but by going to 9.4 tesla and limiting the volume to be studied to a couple of hundred micrometres in thickness, the authors achieve spatial resolutions in the image of the order of 10 to 30 micrometres.

There was much excitement in 1980 when the first clinically useful images of the thorax and abdomen of a patient with multiple cancer deposits were obtained using the technique of NMR imaging[2,3]. This was the realization of a goal first mooted in the early 1970s (refs 4,5) and pursued in several laboratories since then. By 1984 more than 200 machines were being used in hospitals[6], with 15 companies manufacturing them.

Nevertheless, I believe that the full potential of this powerful new imaging technique has still to be realized. What is being imaged is the hydrogen protons of water (and fat) in the body, and the parameters which contribute to the formation of contrast in the image are the proton density (or water concentration); the two magnetic resonance relaxation times t_1 and t_2; and the proton movement. The time t_1 is dependent on the interplay of the water molecules and their macromolecular environment, while t_2 is related to the interplay of the water molecules among themselves, and by carefully choosing the sequence, timing and duration of magnetic-field gradients and radio-frequency pulses one can tailor the image to emphasize one or other of these parameters to emphasize one or other aspect of water use in that tissue being imaged.

Because some of the images show vivid anatomical detail of soft tissue, such as the brain, they are immediately compared by radiologists with the images obtained by the X-ray methods, particularly X-ray tomography or X-ray scanning. Naturally, much effort is now being expended in finding which regions of the body and which disease or which abnormality this new imaging technique is better or worse at than these other existing procedures.

Although this exploratory stage is necessary, it is important not to lose sight of the fact that the signals forming the image are from a quite different source than those from X-rays. The X-ray images are formed by differential absorption of X-rays by the electron clouds of the larger, heavier atoms in the body, whereas these new signals come largely from the nuclei of the hydrogen atoms of the water in the body. The movement of the protons in and out of the imaging volume also influence the signals, and there is now much effort to harness this to show blood flow in major vessels and even to measure the amount of flow, and deviations from it, in these vessels.

No doubt we will now see a rapid exploration of the new NMR instrument described in this issue and a comparison of what it can do with the other microscopic techniques. At first sight this will include the study of material which is alive, and perhaps the really new distinctive feature may be the imaging of the dynamic processes of tissue fluid flow and diffusion. Might not the knowledge gained from the NMR microscope lead us back into attempting to obtain safely a much finer spatial resolution in clinicial images than can be achieved now? Might it also help us to understand the really new contribution of NMR to medicine? □

1. Aguayo, J.B. *et al. Nature* **322**, 190 (1986).
2. Mallard, J.R., Hutchison, J.M.S. *et al. Int. Symp. Med. Radionuclide Imaging* 117 (IAEA, Vienna, 1980).
3. Smith, F.W. *et al. Lancet* **i**, 78 (1981).
4. Damadian, R. *et al. Ann. N.Y. Acad. Sci.* **222**, 1048 (1973).
5. Lauterbur, P.C. *Nature* **242**, 190 (1973).
6. Mallard, J.R. *Proc. R. Soc.* **B226**, 391 (1986).

John Mallard is Professor of Medical Physics at the University of Aberdeen, Aberdeen AB9 2ZD, UK.

Earth sciences

Anoxic oceans and short-term carbon isotope trends

from Wayne D. Goodfellow

THE relationship between catastrophic geological events, mass mortality of species and sudden shifts in carbon isotope levels was demonstrated for the first time at the Cretaceous–Tertiary mass-extinction boundary, where negative $\delta^{13}C$ values (see figure legend) were found to be associated with an iridium anomaly. Similar relationships between platinoid anomalies and short-term carbon fluctuations have been shown at the Permian–Triassic[2], Frasnian–Famennian[3], Precambrian–Cambrian[4] and, most recently, Proterozoic–Palaeozoic[5] boundaries. At other stratigraphic boundaries, a shift in carbon isotope values has been observed with no associated metal anomalies[6]. Many of these changes have been attributed to reductions of the biomass, although other factors may be important.

Changes in carbon isotope values in marine carbonates are influenced by many factors, such the level of mixing of the oceans, fractional preservation of organic matter and biological productivity. Changes in carbon fluxes with time are also important although they are unlikely to explain the relatively short-term and sudden decreases recorded at some System boundaries.

Because living organisms preferentially accumulate carbon-12, an increase of biomass is reflected by a corresponding proportional decrease in the carbon-12 in dissolved carbonate. The converse is also true — a decrease in biological productivity is recorded by an increase in the carbon-12/carbon-13 ratio. Although there is general agreement that perturbations in productivity can generate changes in carbon isotope ratios in carbonates, the cause(s) of these shifts at a particular horizon is often unclear.

The recent data of Magaritz *et al.*[5] were obtained from a section from the Siberian Platform spanning the Proterozoic–

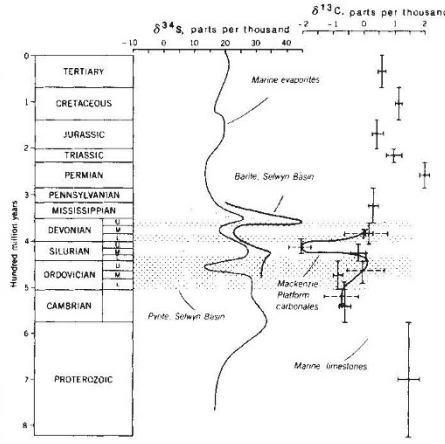

Short-term $\delta^{34}S$ trends in pyrite and barite from the Selwyn Basin[9] and global evaporites[10] and corresponding curves for $\delta^{13}C$ charges in carbonates from the Mackenzie Platform and global carbonate[11]. Small dots, ventilated water column; large dots, water column stratified with anoxic waters.

$$\delta^{13}C = \left[\frac{^{13}C/^{12}C \text{ sample}}{^{13}C/^{12}C \text{ standard}} - 1\right] \times 1{,}000 \text{ parts per thousand}$$

$$\delta^{34}S = \left[\frac{^{34}S/^{32}S \text{ sample}}{^{34}S/^{32}S \text{ standard}} - 1\right] \times 1{,}000 \text{ parts per thousand}$$